JOURNAL OF AGRICULTURAL AND FOOD CHEMISTRY

Article

pubs.acs.org/JAFC

Development of Novel Zein-Sodium Caseinate Nanoparticle (ZP)-Stabilized Emulsion Films for Improved Water Barrier Properties via Emulsion/Solvent Evaporation

Li-Juan Wang,[†,‡] Ye-Chong Yin,[†] Shou-Wei Yin,*[,†] Xiao-Quan Yang,*[,†] Wei-Jian Shi,[†] Chuan-He Tang,[†] and Jin-Mei Wang[†]

[†]Research and Development Center of Food Proteins, Department of Food Science and Technology, South China University of Technology, Guangzhou 510640, PR China

[‡]College of Grain Engineering and Technology, Shenyang Normal University, Shenyang 110034, PR China

ABSTRACT: This work attempted to develop novel high barrier zein/SC nanoparticle (ZP)-stabilized emulsion films through microfluidic emulsification (ZPE films) or in combination with solvent (ethyl acetate) evaporation techniques (ZPE-EA films). Some physical properties, including tensile and optical properties, water vapor permeability (WVP), and surface hydrophobicity, as well as the microstructure of ZP-stabilized emulsion films were evaluated and compared with SC emulsion (SCE) films. The emulsion/solvent evaporation approach reduced lipid droplets of ZP-stabilized emulsions, and lipid droplets of ZP-stabilized emulsions were similar to or slightly lower than that of SC emulsions. However, ZP- and SC-stabilized emulsion films exhibited a completely different microstructure, nanoscalar lipid droplets were homogeneously distributed in the ZPE film matrix and interpenetrating protein−oil complex networks occurred within ZPE-EA films, whereas SCE films presented a heterogeneous microstructure. The different stabilization mechanisms against creaming or coalescence during film formation accounted for the preceding discrepancy of the microstructures between ZP-and SC-stabilized emulsion films. Interestingly, ZP-stabilized emulsion films exhibited a better water barrier efficiency, and the WVP values were only 40−50% of SCE films. A schematic representation for the formation of ZP-stabilized emulsion films was proposed to relate the physical performance of the films with their microstructure and to elucidate the possible forming mechanism of the films.

KEYWORDS: *emulsion films, zein/SC nanoparticles, ethyl acetate, microstructure, physical performance*

INTRODUCTION

Biopolymer-based films have gained interest due to their biodegradability, nontoxicity, and renewability, as a promising substitute for plastic packaging. Physical performances of biopolymer films are usually determined by their chemical nature. Among biopolymer-based films, protein-based films, i.e., sodium caseinate (SC) films, are of benefit owing to their nutritional value and favorable gas resistance.[1] However, their applications are restricted because of poor water resistance and high water sensitivity due to the hydrophilic nature of sodium caseinate[2] since an effective resistance to moisture transfer between packed food and its circumstance is a prerequisite property for food packagings.[3] The incorporation of hydrophobic proteins or lipid may be a potential solution to overcome this drawback of hydrophilic protein films.

Zein, a prolamin, has been utilized to develop delivery vehicles as potential biomaterial usage.[4,5] Zein is a good candidate for fabricating naturally renewable films and/or colloidal particles due to it water-insoluble traits.[6,7] Zein-based materials have specifically interesting properties in terms of water and thermal resistance.[8] In general, zein films are highly fragile,[7,9] which limit their usages in food packaging. Zein can potentially be utilized for edible packagings if its natural brittleness can be improved. Recently, we developed useful films in which zein nanoparticles were *in situ* set down in a SC matrix. This kind of nanostructure provided the films with higher resistance to tensile stress and water vapor transfer than that of SC films and higher ductility than that of zein films.[10] Inclusion of lipid to form composite films may further enhance the water barrier efficiency of zein/SC nanoparticle films.

Usually, emulsion films are good barriers to water vapor transfer. However, the given properties of emulsion films depended on homogenization techniques, lipid content, and/or type, as well as size and distribution of lipid droplets within the films.[11−14] Initial characteristics of emulsions played an important part in the microstructure type and traits of emulsion-based films, and the microstructure of the films determined to a certain extent their physical performances. Various homogenization techniques, e.g., high pressure homogenizer and/or microfluidizer, can be utilized to manipulate the size and distribution of lipid droplets in filmogenic emulsions and film matrices. In a previous research, we utilized a microfluidizer to modulate the lipid droplet distributions of a gelatin−olive oil film-forming solution (FFS) and its film matrix to produce films with improved moisture resistance.[15]

The size and size distribution of lipid droplets of FFS can be further regulated through solvent evaporation methods, following emulsification.[16,17] This emulsification and solvent

Received: July 7, 2013
Revised: October 31, 2013
Accepted: November 1, 2013
Published: November 1, 2013

dx.doi.org/10.1021/jf4029943 | J. Agric. Food Chem. 2013, 61, 11089−11097

evaporation approach has been employed to yield β-carotene nanoparticle dispersions.[18,19] Generally, a volatile organic phase is apart from the emulsions by a rotary evaporation approach, causing the lipid droplets to shrink.[20] Ethyl acetate, an amphiphilic volatile organic solvent, has been widely utilized to produce nanoemulsions in the pharmaceutical industry,[21] and it has been conferred GRAS status (generally recognized as safe) by the US FDA when incorporated in foods and beverages.[20] Food-grade whey protein-stabilized nanoemulsions had come into being by an approach in which the ethyl acetate evaporation process was performed after high energy emulsification (high pressure homogenization).[20] However, few works were performed to yield emulsion films via the combination of microfluidic emulsification and solvent evaporation techniques.

Stabilization phenomena against creaming or coalescence during film drying played a crucial part in the physical performance of formed emulsified films. The nature of the repulsive interactions between lipid droplet surfaces determines the coalescence stability of formed emulsion, and the primary influence on the range of the inter droplet repulsive interactions is the thickness of the stabilizing layer.[22] The absorption of zein nanoparticles at the oil−water interface may increase the thickness and strength of the interface layer, thus preventing droplet flocculation and coalescence during the cast process by a steric mechanism, producing novel nanoparticle-stabilized emulsion films with improved physical performance. Therefore, the aim of this research is to prepare edible ZP-stabilized emulsion films with high moisture barrier efficiency. Microfluidic emulsification alone or in combination with solvent (ethyl acetate) evaporation was used to prepare the FFS. Some selected physical properties, including mechanical and optical properties, water vapor permeability (WVP), and surface hydrophobicity, along with the microstructure of the films were evaluated. A schematic representation of the formation pathway of ZP-stabilized emulsion films was proposed to correlate the physical performances of emulsion films with their microstructure. Finally, the possible forming mechanism of these films will be discussed.

MATERIALS AND METHODS

Materials. Ethyl acetate was purchased from Sinopharm Chemical Reagent Co. Ltd. (Shanghai, China). Zein (product no. Z 3625) was obtained from Sigma Chemical Co. (St. Louis, MO, USA). Corn oil was obtained in a local supermarket (Guangzhou, China). Food-grade sodium caseinate (SC) was obtained from Murray Goulburn Co-operative Co. Limited (Southbank Victoria, Australia). Other chemicals were of analytical grade.

Solution Preparation. An aliquot of 2.5 g of zein powder was dispersed in 100 mL of 80:20 ethanol−water (v/v) solutions to obtain the zein stock solution. SC dispersions were produced by adding 1.0 g of SC powder to 100 mL of deionized water, and the resultant SC solutions were magnetically stirred overnight to facilitate SC hydration. Organic phase for the zein nanoparticle (ZP) stabilized emulsion (ZPE) and SC stabilized emulsion (SCE) consisted of 100% corn oil, whereas for the film-forming emulsion, the organic phase comprised 10% corn oil and 90% ethyl acetate produced by using the combination of microfluidic emulsification and solvent evaporation approach (ZPE-EA).

Particle Synthesis. ZP was fabricated via a so-called antisolvent procedure. All operations were at room temperature. Zein solution was trickled into the SC solution within 2 min under continued shearing (10000 rpm) using an Ultraturax T25 homogenizer (Janke & Kunkel, Germany). The SC-to-zein weight ratio was 1:1. After shearing for another 10 min, the remaining ethanol in ZP dispersions was removed by using an RV 10 digital rotary evaporator (IkA-Works Inc., Germany). Then, the dispersions were centrifuged at 2000*g* for 10 min to get rid of some insoluble aggregates. Particle size, shape, and ζ-potential of fresh ZP dispersions were characterized prior to the casting process. Finally, the obtained ZP dispersions were utilized to produce FFS.

Preparation of Film-Forming Solutions. After the inclusion of the oil phase, the coarse emulsions were produced by an Ultraturax T25 homogenizer (Janke & Kunkel, Germany) at 5000 rpm for 2 min, and the operation was performed in an ice bath to avoid ethyl acetate evaporation. Then, the coarse emulsions were further processed by a M-110EH Microfluidizer (Microfluidics International Corp., Newton, Massachusetts, USA) for 2 passes at 50 MPa pressure to yield fine emulsions. Ethyl acetate was vaporized from ZP-stabilized emulsions using an RV 10 digital rotary evaporator (IkA-Works Inc., Germany) for 20 min at 50 °C. Finally, ZP-stabilized emulsions contained about 0.9 wt % SC, 0.9 wt % zein, and 0.9 wt % corn oil. SCEs were produced by the same procedure as that mentioned above.

Preparation of Films. After mixing with glycerol at a glycerol-to-protein ratio of 0.3:1, the ZP dispersions or ZP-stabilized emulsions were poured into polyethylene-coated glass plates (18 × 20 cm) and dried for 48 h in a thermostatic chamber in which the temperature and relative humidity (RH) was set at 25 ± 1 °C and 50 ± 5%, respectively. Finally, the films were taken off from glass plates. In each plate, the thickness of the films was regulated by using the FFS with the same solid content (3.24 g). The obtained films were equilibrated for 2 days in a desiccator at 25 °C and RH 58 ± 3% prior to the trials.[23]

Film Thickness. Thicknesses of ZP and ZP-stabilized emulsion films were determined using a digital micrometer (with 0.001 mm sensitivity). Film thickness used in tensile strength calculations were measured along the length of film strips, whereas films thicknesses at five random points of circular film disks were measured for calculating WVP.

Light Transmittance. The UV−visible spectra of the films were recorded from 250 to 700 nm in a UV−visible spectrophotometer (UV-2300, TianMei Techcomp Limited., Shanghai, China).

Water Vapor Permeability (WVP). WVP of the films were tested according to a modified approach of the ASTM E96-95 gravimetric method.[24,25] Circular film disks with a diameter of 6 cm were used for WVP testing, and these circular films were free of physical defects. Circular cups of 4.5 cm in diameter and 3 cm in height were utilized for WVP testing. In brief, 15 mL of deionized water was put in each cup to maintain 100% RH, and then film specimens were fixed on the opening of a cup using paraffin. Once the films were secured, the cups were placed in a desiccator with 0% RH where a fan was utilized to maintain the RH uniformity within the whole desiccator. After being left at equilibrium for 2 h, we took the cups out and weighed them periodically by an analytical balance (with 0.1 mg precision) at about 3 h intervals. Water vapor transfer was measured by the weight loss of the cup. WVP of the films was calculated according to the following equation:

$$\mathrm{WVP} = \Delta m \times L/(A \times \Delta t \times \Delta P) \quad (1)$$

where Δm is the weight loss (g) of the cups during the test time Δt (h). L is film thickness (mm), A is the exposed area of films (m^{-2}), and ΔP is the partial water vapor pressure (kPa).

Mechanical Properties. Mechanical Properties of the films were determined according to the ASTM standard method (D882) using a TA-XTplus texture analyzer (SMS Ltd., London, U.K.).[26] The trials were performed in a tensile mold using an A/TG tensile grip. The texture analyzer was calibrated using a 5 kg counterweight before the test. In tensile testing, initial distance between grips and test speed were set at 50 mm and 1 mm/s, respectively. Tensile parameters, including tensile strength (TS), elastic modulus (EM), and elongation at break (EAB), were computed from the stress−strain curves using the Texture Exponent 32 software. The tensile testing for each film was performed at least eight times, and the means were taken as the experimental result.

Contact Angle Measurements. Water contact angle was utilized to represent the surface hydrophobicity of the films. Contact angle measurements were performed according to the sessile drop method, using an OCA 20 AMP (Dataphiscis Instruments GmbH, Germany) equipped with a high-speed video camera. An aliquot of 4 μL of Milli-Q water was deposited on the surface of the films using a high-precision injector. The drop image was photographed using a high-speed video camera at a rate of 10 pictures per second, and the LaPlace–Young equation was used to fit the profile data of the droplet. Ten tests were carried out for each film.

Atomic Force Microscopy (AFM). AFM technique was utilized to analyze the surface topography of the films. The trial was performed at room temperature using multimode scanning probe microscopes (SPM) (Veeco Instruments, Plainview, NY, USA) operated by a Nanoscope IIIa controller. Square filmstrips with dimensions of 2.5 × 2.5 mm^2 were fixed on mica disks using double-sided tape. AFM photos (10 × 10 μm^2) of the films were obtained using the tapping mode on their air side. Surface roughness parameters (R_q and R_a) of the films were calculated using the NanoScope software, version 5.12, according to the standard ASME B46.1.14.

Confocal Laser Scanning Microscopy. CLSM experiments were performed according to the procedure of Ma et al.,[27] using a Leica TCS SP5 CSLM (Leica Microsystems Inc., Heidelberg, Germany). Various specimens of emulsion films were dyed with a mixed fluorescent dye solution consisting of 1 mg mL^{-1} Nile Red and 1 mg mL^{-1} Nile Blue A (in isopropyl alcohol). The dyed films were placed on concave slides, then the concave slides were covered with coverslips. Finally, glycerol was coated around the coverslips to seal the samples. The fluorescent dyes were excited by an argon laser at 488 nm for Nile Red (labeling oil) and a Helium Neon (He–Ne) laser at 633 nm for Nile blue A (labeling protein). CLSM images of emulsion films were acquired between 5 and 30 μm penetrations under the surface of the air side, at 2 μm intervals.

Statistics. Statistical analyses were performed using an analysis of variance (ANOVA) procedure of the SPSS 13.0 statistic analysis program, and the differences between means of the trials were detected by a least significant difference (LSD) test ($P < 0.05$).

RESULTS AND DISCUSSION

Particle Size Characterization of the FFS. Figure 1 shows the typical droplet size distribution of various FFS. The

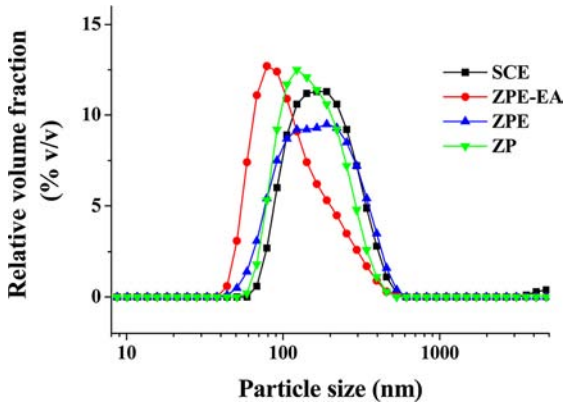

Figure 1. Particle size distribution of the film-forming solution (FFS), as a function of film-forming approaches.

FFS produced by ZP dispersions showed a nearly monomodal droplet size distribution, and the position of the maxima appeared at about 120 nm (Figure 1). The particle size distribution of FFS was dependent on film-forming techniques, and the type of stabilizers. The addition of oil changed the particle size distribution of the FFS from a nearly narrow monomodal (ZP) to broad pattern (ZPE), and the major peak shifted to large particle size. The FFS recovered a narrowly monobimodal particle size distribution when the solvent (ethyl acetate) evaporation approach was used, and the peak moved to low droplet size (Figure 1). This phenomenon was attributed to ethyl acetate evaporation-induced shrinkage of lipid droplets (Figure 1). A similar phenomenon was observed in whey protein isolate (WPI)-stabilized nanoemulsions using ethyl acetate and corn oil as organic phase.[20] Similarly, SCE, as the control, exhibited a monomodal particle distribution, with the maxima at about 150 nm.

Concomitantly, the mean particle size was used to quantitatively characterize the FFS, reflecting that all preparations were nanoscalar. As expected, the average droplet size of ZP dispersions was 154.3 ± 1.4 nm. The incorporation of corn oil caused the particle size of FFS to increase to 161.9 ± 6.3 nm (ZPE). As expected, the ethyl acetate (solvent) evaporation approach reduced the particle size of the FFS to 128.9 ± 1.2 nm (ZPE-EA). Zeta potentials of various filmogenic solutions ranged from −30 mV to −33 mV (Table 1), implying strong electrostatic repulsion among the nano-

Table 1. Mean Particle Size and Z-Potential Values for Film-Forming Solutions as a Function of Filmogenic Approach

film type	particle sizes (nm)	zeta-potential (mV)	PDI
SCE[a]	172.4 ± 0.5	−32.8 ± 0.5	0.16 ± 0.01
ZP[b]	154.3 ± 1.4	−30.2 ± 0.1	0.11 ± 0.01
ZPE[c]	161.9 ± 6.3	−32.2 ± 0.1	0.14 ± 0.01
ZPE-EA[d]	128.9 ± 1.2	−30.4 ± 0.2	0.16 ± 0.01

[a]SCE: sodium caseinate emulsion (SCE) films. [b]ZP: zein nanoparticles (ZP) films. [c]ZPE: ZP stabilized emulsiong films. [d]ZPE-EA: ZP emulsion films via the ethyl acetate evaporation approach.

particles in the FFS. The mean diameter data further supported the hypothesis that the size of the FFS produced by the microfluidizer can be further reduced via the solvent evaporation approach. Initial characteristics of the FFS would influence to some degree the microstructure of emulsion films, and the microstructure of the films plays a key role in the physical performance of the films.

Visual Appearance and Light Absorption. *Visual Appearance.* SC alone films were rather transparent, whereas SC-stabilized emulsion films became translucent and milky (Figure 2A). Additionally, a little lipid droplet was clearly confirmed on the air side of the SCE film via direct handling by hand. Similar observations were reported by Pereda et al.[13] This phenomenon was attributed to destabilization phenomena like creaming during the formation of the SCE film. The relatively weak stability against coalescence or the creaming phenomenon, for SC-stabilized film-forming solutions, may partially account for the emergence of oil droplets at the surface of SCE films. Interestingly, no obvious lipid droplets were sensed for ZPE and ZPE-EA films on their surfaces when we dealt with them, reflecting that ZP-stabilized film-forming emulsions possessed high physical stabilization during film formation. Visually, both ZPE and ZPE-EA films were slightly yellow, with homogeneous and compact structure. ZPE films were translucent, whereas ZPE-EA films were transparent (Figure 2A). This result was in accordance with quantitative transmittance of the films at the visible regions, also evidenced by the internal microstructure trait of the films.

Light Absorption. Transparency is a paramount parameter in edible food packaging, owing to its direct effect on the

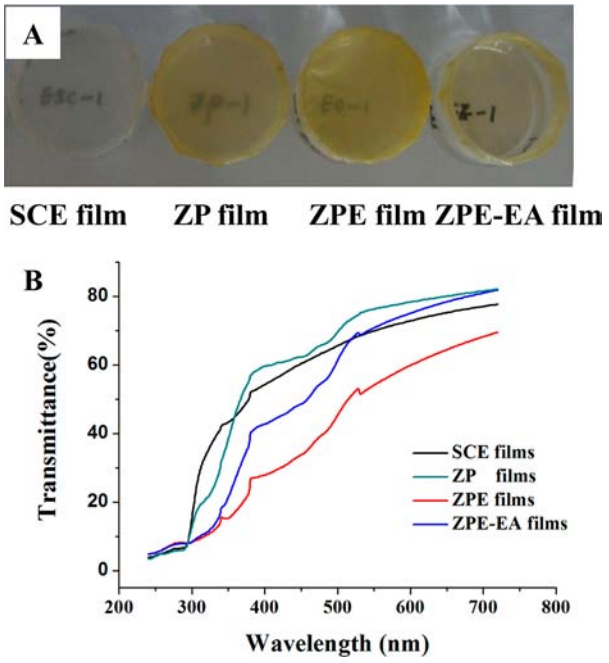

Figure 2. Visual appearance (A) and UV−vis spectra (B) of the films produced by various film-forming approaches. SCE films: sodium caseinate emulsion films. ZP films: zein nanoparticles films. ZPE films: ZP emulsion films. ZPE-EA films: ZP emulsion films via ethyl acetate evaporation approach (ZPE-EA).

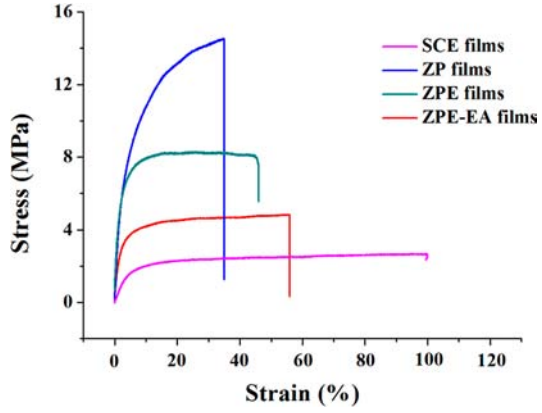

Figure 3. Representative stress−strain curves of the films as a function of film-forming approaches.

Table 2. Tensile Properties of the Films as a Function of Filmogenic Approach[a]

film type	EM (MPa)	TS (MPa)	EAB (%)
SCE	67.8 ± 29.5 c	2.7 ± 0.1 d	110.1 ± 9.9 a
ZP	312.5 ± 40.0 a	13.6 ± 1.4 a	29.0 ± 4.9 c
ZPE	296.0 ± 76.9 a	7.4 ± 1.3 b	45.7 ± 8.6 c
ZPE-EA	175.4 ± 15.2 b	4.7 ± 0.5 c	54.5 ± 3.2 b

[a]Values were expressed as the means and standard deviations of eight measurements. Superscripted letters (a−d) indicate significant ($P < 0.05$) difference within the same column.

appearance of wrapped products. Figure 2B shows the spectral distribution of the transmittance (Ti) of the films. The films presented different light transmission profiles in the visible (350−700 nm) ranges, whereas all preparations exhibited a similarly low light transmission in the UV (250−350 nm) range. The addition of lipid (ZPE films) produced a sharp decrease in the transmittance of ZP films in the visible region, whereas ZPE-EA films became more transparent (Figure 2B). In general, the dispersed droplets (nonmiscible phase) within the film matrix bring an increase in film opacity as a result of the discrepancy in the refractive index of the dispersed and continuous phases. Droplet size and concentration of the dispersed phase play a key role in film opacity that is in fact a function of the differences of the refractive index between both phases.[13,28] Nano lipid droplets were uniformly distributed in the matrix of ZPE films. In contrast, both oil and protein phases were overlapped to form a uniform microstructure within the ZPE-EA films, confirmed by CLSM images. These structural attributes account for the difference in film transparency.

Mechanical Properties. Generally, mechanical resistance and ductility are very important parameters for packaging films which should possess external stress tolerance and maintain its integrity during transportation and strorage.[3] Figure 3 shows representative stress−strain curves of ZP emulsion films, with SCE films as the control. We fabricated novel films in which zein nanoparticles were in situ set down in a SC matrix. As a consequence, this novel nanostructure provided the films with higher resistance to tensile stress and water vapor transfer than the SC film and higher ductility than the zein film.[10] ZP films exhibited improved tensile properties when compared with those of our previous research, which may be attributed to the different processing procedures.

Table 2 shows the tensile strength (TS), elastic modulus (EM), and elongation at the break (EAB) of the films calculated from the above-mentioned stress−strain profiles. The calculated TS, EM, and EAB values of the ZP films were 13.6 ± 1.4 MPa, 312.5 ± 40.0 MPa, and 32.7 ± 8.5%, respectively. The incorporation of corn oil in film formulations resulted in an increase in EAB and a decrease in EM and TS. The TS of the films gradually reduced from 13.6 MPa to about 7.4 MPa for ZPE films and 4.7 MPa for the ZPE-EA films. Concomitantly, the EAB of the films presented an increased trend, from 29.0%, to 45.7% and 54.5%, respectively. The plasticizing effect of lipid on the films may account for this phenomenon. In general, an emulsion film is more extensible than a control film without oil. This phenomenon can be associated with the deformability of lipid droplets within the film matrix, evidenced by the fact that lipid droplets are easily deformable during the tensile process. Atarés et al. reported similar results where cinnamon oil exerted plasticizing effects on the soy protein isolate (SPI) films, yielding outstretched SPI-stabilized cinnamon oil emulsion films.[11] When incorporated into the solvent evaporation procedure, this plasticizing effect was further intensified. The formation of interpenetrating protein−oil complex networks within ZPE films may to a certain extent account for this phenomenon. In contrast, the SC-stabilized emulsion films were more extensible but showed less mechanical resistance.

Moisture Content (MC). The absorption isotherms of the films are shown in Figure 4. It was clear that all tested films had a high moisture absorption rate at the initial 0−6 h, and that equilibrium was reached after approximately 6 h of absorption. Equilibrium moisture content (EMC) of the films depended on film compositions. The EMC of the films decreased from about 22.0% (ZP films) to 15.5% due to the inclusion of corn oil, whereas ZPE and ZPE-EA films have a similar EMC value, and this EMC value was less than that of the counterpart of SCE films (about 17.8%) (Figure 4). The aforesaid result may be

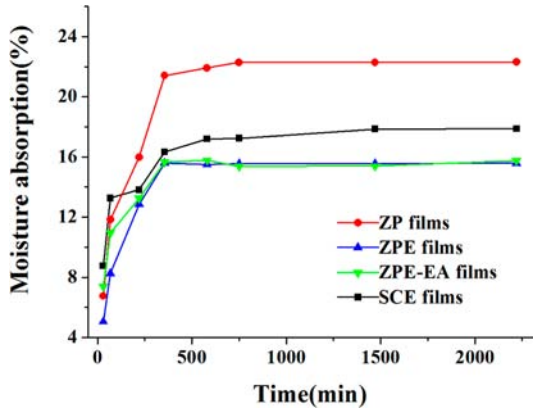

Figure 4. Water vapor absorption of the films produced by various processes.

due to the in situ formation of zein nanoparticles (ZP), a hydrophobic particle, within the films matrix.

Water Vapor Permeability. The homogeneous distribution of lipid droplets benefit the barrier of emulsion films to moisture transfer, and the smaller the lipid droplets, the lower is the WVP.[14] Table 3 shows the WVP of the films. The WVP of ZP films was 2.07 ± 0.06 g mm kPa^{-1} m^{-2} h^{-1} and slightly lower than that of the counterpart of SC films (Table 3). Corn oil inclusion within the ZP matrix yielded ZP-stabilized emulsion films with improved water resistance. In detail, the WVP of the films decreased from 2.07 ± 0.06 to 1.15 ± 0.08 and 0.93 ± 0.06 g mm kPa^{-1} m^{-2} h^{-1} for ZPE films and ZPE-EA films, respectively. Interestingly, both ZP-stabilized emulsion films exhibited a better water barrier efficiency when compared with that of SCE films, and the WVP of these films was only 40−50% of SCE films at the same lipid content. The possible rearrangement of oil droplets during film network formation, resulting in different microstructures for the films, may account for this discrepancy.

Table 3. Water Contact Angle and Water Vapor Permeability of the Films[a]

film type	contact angle (deg)	WVP g mm kPa^{-1} m^{-2} h^{-1}
SC		2.21 ± 0.15 a
SCE	73.5 ± 1.3 b	1.95 ± 0.03 c
ZP	79.7 ± 5.4 ab	2.07 ± 0.06 b
ZPE	86.3 ± 2.8 a	1.15 ± 0.08 d
ZPE-EA	78.3 ± 8.8 ab	0.93 ± 0.06 e

[a]Values were expressed as the means and standard deviations of eight measurements. Superscripted letters (a−e) indicate significant (P < 0.05) difference within the same column.

The stability of filmogenic emulsion during the drying step plays a key role in influencing the physical performances of emulsion films. In the case of conventional protein-stabilized emulsion films, the initial droplet size and size distribution of the FFS will change due to the creaming and coalescence behavior of lipid droplets during film formation (FFS drying process). In some cases, an "apparent bi-layer structure" is observed on the surface (air side) of emulsion films, thus causing the films to be a more effective barrier to water transfer.[29,30] However, the moisture resistance of the films may be similar to the hydrophilic hydrocolloid matrix if the aforementioned apparent bi-layer structure does not appear. A few lipid droplets were clearly confirmed on the air side of the SCE film via direct handling by hand, but it did not form an analogous protein−lipid bilayer structure. In addition, the distribution of lipid droplets was not homogeneous along the cross-section from the air side to the interior of the films, and the density of lipid droplets decreased. In other words, the lipid phase was rich in the near-surface region of the films. In fact, the hydrophilic SC matrix played crucial role in the barrier performance of SCE films in view of the microstructure character of the obtained SCE films, and the WVP decreased only by about 10% from 2.21 (SC films) to 1.95 ± 0.03 (SCE films) g mm kPa^{-1} m^{-2} h^{-1}. Similarly, the inclusion of hydrophobic oleic acid and stearic acid only slightly decreased the WVP of SC films.[12]

When oil is incorporated within the ZP matrix, the WVP of the films presented a completely different response. It decreased by 44−55% compared with that of ZP films. Generally, the decrease of lipid droplet size in the FFS was well correlated with the reduction of water vapor permeability.[14] The mean droplet size of various FFS was in the range of 128 and 172 nm, and so a small difference in the initial lipid droplets of FFS was insufficient to yield so big a difference in water vapor permeability among the films. The unique stabilization phenomena of ZP-stabilized film-forming emulsion via the particle stabilization mechanism against creaming or coalescence during film network formation may contribute to the high water resistance of the formed films.

In the case of ZPE films, the absorption and accumulation of zein nanoparticles on the lipid droplet surfaces produced thick and firm interface layers as a steric hindrance, which protected lipid droplets from creaming and coalescence during film network formation. Though the mild density gradient of lipid phases was confirmed for ZPE films from the near-surface to the interior, individually nanoscalar lipid droplets were still uniformly distributed within the interior of the film matrix. Thus, the microstructure of ZPE films was characterized by the presence of small but more numerous interruptions in the continuous hydrophilic matrix by hydrophobic lipid droplets. Interestingly, this kind of nanostructure increased the tortuosity factor against moisture transfer. As a result, the structural characteristics endowed ZPE films with a strong barrier to water transfer.

In the case of ZPE-EA films, ethyl acetate evaporation, following microfluidic emulsification, was utilized to modulate lipid droplet size and size distribution of the FFS and film matrices. This strategy may facilitate the migration of zein nanoparticles toward the oil−water interface and the accumulation at lipid droplet surfaces. Meanwhile, the shrinking phenomenon of lipid droplets after ethyl acetate evaporation may result in the increased density of zein nanoparticles on the lipid droplet surface. The thick and firm ZP-stabilized interface structure may prevent droplet flocculation and coalescence by a steric mechanism during film network formation. Interestingly, the green (oil phase) and red (protein-rich phase) phases overlapped to form a light yellow phase within the matrix of ZPE-EA films, reflecting the formation of interpenetrating protein−oil complex networks. The structural characteristics gave the films strong water barrier capability.

Surface Hydrophobicity. Water contact angle is a measure of the basic wettability of packaging materials, and the relative terms "hydrophobic" and "hydrophilic" surfaces have been defined based on a water contact angle $\theta > 65°$ and $\theta < 65°$, repectively.[31] In this work, the initial contact angle when a drip is just deposited onto the film surface was utilized to evaluate

the surface hydrophobicity of the films. Table 3 displays the contact angles (θ) of Milli-Q water on the surface of various films. The water contact angle of emulsified films ranged from 73.0 to 86.3°, depending on the composition of the films. The present data indicated that the tested films, including ZP, ZPE, and SCE films possessed hydrophobic surfaces. This result can be related with the high surface roughness for these films.

Film Microstructure. *CLSM.* The morphological structure of emulsion films, including lipid droplet size and size distribution within the film matrix, determined to some degree their physical performances. It can be evaluated by the CLSM technique via the combination of electronic microscopy and fluorescence labeling. The CLSM images of the films are shown in Figure 5. Emulsion films exhibited remarkable differences in morphological structure, in a type of stabilizer- and processing-procedure-dependent manner. In addition, the microstructure character of the films also depended on scanning position within the films (Figure 5). The microstructures of ZP films were homogeneous, but phase separation of lipid and protein was visible for SCE and ZPE films in which these emulsion films presented continuous protein microstructures. Within these film matrices there were protein-rich (red) phases and lipid-rich (green) phases, and the lipid (green) seemed to be inserted in the protein network (Figure 5B,C). Interestingly, the green (oil phase) and red (protein-rich phase) phases overlapped to form a light yellow phase within ZPE-EA films, and the films were characterized by the formation of interpenetrating protein−oil complex networks (Figure 5D).

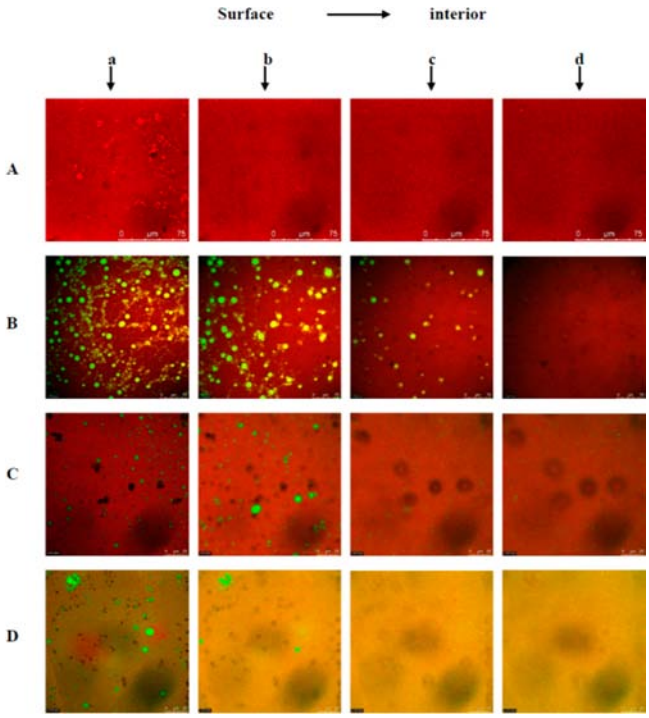

Figure 5. Selected CLSM images of the films produced by various processes as a function of penetration depth. Panel A: zein nanoparticle (ZP) films. Panel B: sodium caseinate (SCE) films. Panel C: ZP emulsion (ZPE) films. Panel D: ZP emulsion films via the ethyl acetate evaporation approach (ZPE-EA). The film was stained by Nile Blue A and Nile Red; red and green indicate protein-rich phase and oil phase, respectively. (a) 5 μm; (b) 11 μm; (c) 21 μm; and (d) 28 μm.

In the case of SCE films, the occurrence frequency of lipid droplets showed a decreasing tendency along the transverse surface from the near-surface of the air side to the interior of the films, supporting the hypothesis that oil phases were rich in the near-surface region of SCE films. That is, the sign of the oil phase gradually weakened when the scanning position shifted to the interior of the films (Figure 5B). In the case of ZPE films, the films displayed a slight density gradient for lipid droplets within th enear-surface region of the films, but the visibly nanoscalar oil phase (green) was homogeneously distributed within the interior of the films (Figure 5B). The unusual stabilization of the FFS during th ecasting process may account for this phenomenon, which may be partially associated with the particle-like stabilization mechanism. During the formation of emulsion, zein nanoparticles migrated toward the oil−water interface and accumulated on lipid droplet surfaces to form steric hindrance that protected lipid droplets in the FFS against flocculation and coalescence. This is why the ZP-stabilized FFS were more stable than SC FFS against creaming during the film formation process (casting step).

In the case of the ZPE-EA film, the green (oil phase) and red (protein-rich phase) phases overlapped to form uniform interpenetrating protein−oil complex networks, showing a light yellow phase in the CLSM image. The underlining rule for the formation of the preceding fascinating nanostructure was unknown, but it may be attributed to the interaction between the protein and oil phases to form a oil−protein complex. The incorporation of ethyl acetate may facilitate ZP to migrate toward the oil−water interface and then accumulate on the lipid droplet surface, leading to thicker interface layers when compared with that of the classic SC emulsions, with strong mechanical barriers against creaming via a steric mechanism. Meanwhile, ethyl acetate evaporation caused the oil droplets to shrink, resulting in the increased density of zein nanoparticles at the lipid droplet surfaces. Finally, the formation of the uniformly interpenetrating protein−oil complex via a thick interface layer (protein), nanoscalar lipid droplets, and the residual zein nanoparticles, accounted for the unique microstructure of ZPE-EA films.

AFM. Surface morphology of the films was investigated by the AFM technique. The three-dimensional AFM images were acquired for the height of the films relative to a reference plane. Figure 6 shows typical AFM images of various films. ZP films showed surface topographies with apparent peak and valley interlacements. Clearly, oil incorporation in the film formulations distinctly changed the surface topographies of the films, producing a decreasing surface roughness for ZPE films (Figure 6). Roughness parameters (R_q and R_a) were calculated using the NanoScope software, version 5.12, to quantitatively reflect the alteration in surface topographies of the films. R_q refers to the mean size of peaks and valleys within the tested area. Lower R_q values reflect an even surface. The R_q diminished from 110.2 to 17.8 ± 2.0 (ZPE films) or 26.9 ± 6.3 (ZPE-EA films). The average roughness (R_a) presented a similar trend (Table 4). This present data indicated that emulsion films have a relatively lower surface roughness with regard to oil-free films. This phenomenon may be principally ascribed to the presence of free oil that released from dispersed emulsion droplets during the drying stage of the FFS. Such trends were in accordance with the coagulation and coalescence behavior of lipid droplets when the drying takes place on film surface. Atarés et al. reported similar varieties in surface properties of sodium caseinate films upon adding ginger oil.[12]

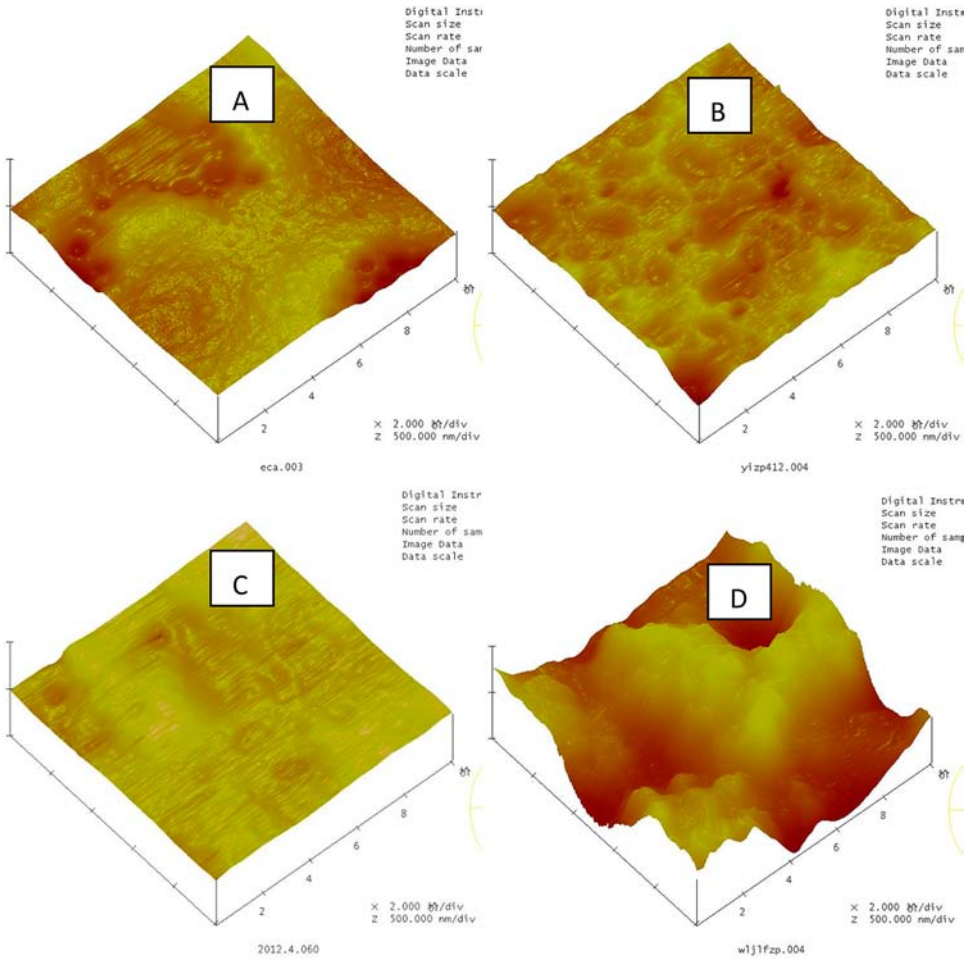

Figure 6. AFM images for the films as a function of the filmogenic approach (scaning scale, 10 μm; height scale, 100 nm). Panel A: ZPE-EA film. Panel B: ZPE films. Panel C: ZP films. Panel D: SCE films.

Table 4. Roughness Parameters Obtained from AFM Analysis of the Films as a Function of the Filmogenic Approach[a]

film type	R_q[b]	R_a[c]
SCE	10.2 ± 2.1 c	6.4 ± 1.0 c
ZP	110.2 ± 12.8 a	89.0 ± 6.3 a
ZPE	17.8 ± 2.00 c	13.4 ± 1.71 c
ZPE-EA	26.9 ± 6.3 b	20.8 ± 5.0 b

[a]Values were expressed as the means and standard deviations of eight measurements. Superscripted letters (a–c) indicate significant ($P < 0.05$) difference within the same column. [b]R_q: root-mean-square roughness. [c]R_a: average roughness.

Schematic Illustration. The WVP values of ZPE and ZPE-EA films were 1.15 ± 0.08 and 0.93 ± 0.06 g mm kPa^{-1} m^{-2} h^{-1}, respectively, and these values were 40–50% of SCE films, reflecting that ZP-stabilized emulsion films had favorable water vapor barrier efficiency. These phenomena suggesting the possible flocculation and coalescence of lipid droplets during film network formation played a key part in the microstructure of emulsion films. However, the microstructure of the films may have a determining role in the physical performance of formed films.

Herein, a schematic diagram for the formation pathway of ZP-stabilized emulsion films is proposed, to correlate the physical performance of emulsion films with their microstructure, so as to elucidate the possible mechanism for excellent water vapor barrier efficiency for ZP-stabilized emulsion films (Figure 7). In the case of SCE films derived from conventional SC-stabilized film-forming emulsion, this kind of FFS was labile to creaming or coalescence. During the drying of SCE, water evaporation gave rise to the condensation of SCE, with subsequent reduction in droplet–droplet distance; as a result, the initial SCE structure will be changed, particularly driven by creaming, flocculation, or coalescence.[30,32] Thus, the films showed a visible gradual density decrease of lipid phases along the transverse surface from the near-surface of the air side to the interior of the films, indicating that the oil phase was rich in the near-surface region of SCE films (Figure 4A). Furthermore, the existence of free corn oil on the air side of the SCE film was clearly confirmed via direct handling by hand. However, the apparent protein-lipid bi-layer structure was not formed; therefore, the barrier to moisture transfer for SCE films is similar to that of the hydrophilic SC films due to the apparent enrichment of oil at the near-surface region of the films. Therefore, the WVP of the films decreased slightly by about 10% from 2.21 to 1.95 g mm kPa^{-1} m^{-2} h^{-1} (Table 3).

The high resistance against creaming or coalescence is a major benefit of particle-stabilized emulsion. In general, the energy barrier for particle desorption is higher than the kinetic energy of Brownian motion, which makes the adsorption effectively irreversible.[33] Thus, particle-stabilized emulsion (via a Pickering-like mechanism) may exhibit unique stabilization

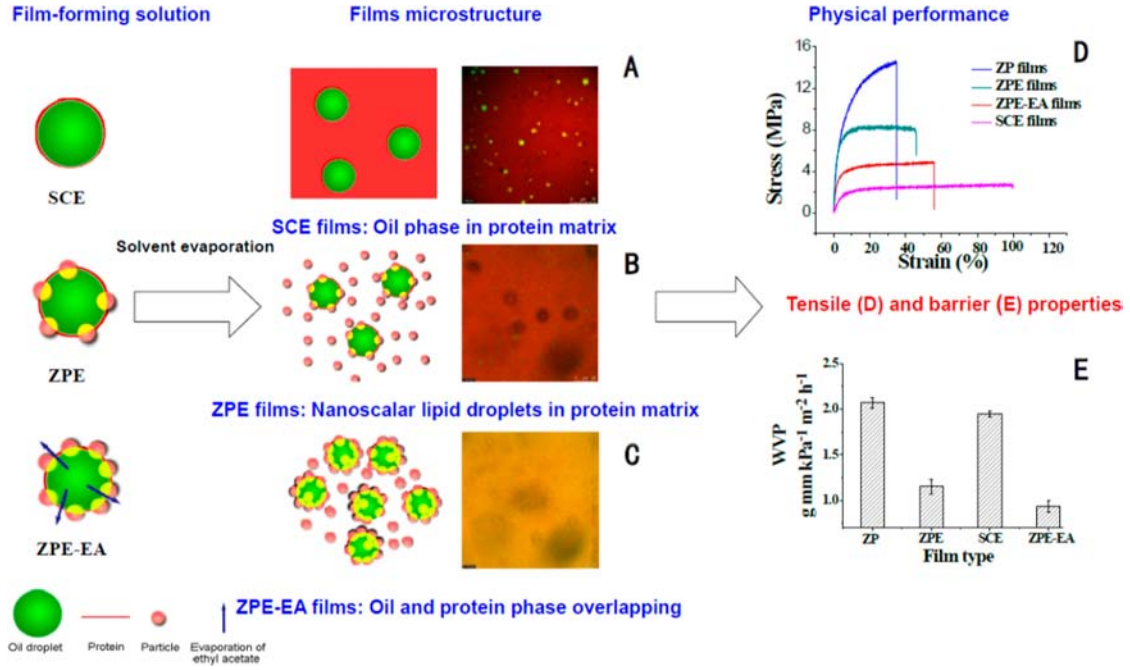

Figure 7. Schematic illustration of the formation pathway of ZP-stabilized emulsion films via the emulsion/solvent (ethyl acetate) evaporation approach.

during drying (film formation), producing a novel microstructure.

In the case of ZPE films in which zein nanoparticles were used to stabilize corn oil to fabricate particle-stabilized emulsion films via a Pickering-like stabilization mechanism. The absorption and accumulation of zein nanoparticles on lipid droplet surfaces may strengthen the interface layer, producing a strong mechanical barrier that protected lipid droplets of ZPE against coalescence and creaming during film network formation. Though ZPE films displayed a slight density gradient for lipid droplets within the near-surface region of the films (Figure 1), individual nanoscalar lipid droplets were still at uniform distribution within the interior of the film matrix (Figure 7B). The structural characteristics endowed the films with strong water barrier capability and moderate mechanic resistance and extensibility.

In the case of ZPE-EA films, the emulsion/solvent (ethyl acetate) evaporation approach was used to tune lipid droplet size and size distribution of ZPE-EA and the films. The incorporation of ethyl acetate in the dispersed oil phase may accelerate the migration of ZP toward the oil−water interface to produce steric hindrance among lipid droplets of ZPE-EA. Meanwhile, the removal of ethyl acetate via evaporation caused lipid droplets to shrink, resulting in the increased density of ZP at the oil−water interface. The thick ZP-stabilized interface layers are more effective in preventing droplet flocculation and coalescence by a steric mechanism. Therefore, this kind of FFS was very stable during film network formation. Interestingly, the green (oil phase) and red (protein-rich phase) phases overlapped to form a light yellow phase within the matrix of ZPE-EA films, reflecting the formation of interpenetrating protein−oil complex networks within the films (Figure 7C). The structural characteristics gave the films improved water barrier capability, moderate mechanical resistance and extensibility, and high transparency.

Conclusions. Novel ZP-stabilized emulsion films were fabricated via microfluidic emulsification or in combination with solvent (ethyl acetate) evaporation techniques to enhance the water resistance of protein-based films. Both ZP-stabilized emulsion films exhibited a better water barrier efficiency, and the WVP of ZPE and ZPE-EA films was only 40−50% of SCE films. The absorption and accumulation of zein nanoparticles on the droplet surfaces resulted in a steric barrier, which contributed to the unique stabilization of ZP-stabilized film-forming emulsion. Nano lipid droplets were homogeneously distributed within the ZPE film matrix, and oil and protein phases were overlapped to form interpenetrating protein−oil complex networks within the ZPE-EA films. In contrast, SCE films presented a heterogeneous microstructure with an apparent compositional gradient. The structural characteristics of ZP-stabilized emulsion films gave them excellent physical performance, especially water barrier capability. In particular, the ZPE-EA films showed optimally improved water barrier capability, transparency, and mechanical flexibility. In all, the combination of particle stabilization mechanism and solvent evaporation techniques produced unique emulsion films with excellent physical performance.

AUTHOR INFORMATION

Corresponding Authors

*(S.W.Y.) Phone: +86-2087114262. Fax: +86-20-87114263. E-mail: feysw@scut.edu.cn.

*(X.Q.Y.) Phone: +86-2087114262. Fax: +86-20-87114263. E-mail: fexqyang@scut.edu.cn.

Funding

This work is partially supported by The Project Supported by Guangdong Natural Science Foundation (S2013010012097). We also appreciate the financial support by the Fundamental Research Funds for the Central Universities (SCUT, 2012ZZ0082), Key Projects in the National Science & Technology Program during the Twelfth Five-year Plan Period (2013BAD18B10-4) and National Natural Science Foundation of China (31271885).

Notes

The authors declare no competing financial interest.

REFERENCES

(1) Ou, S. Y.; Kwok, K. C.; Kang, Y. J. Changes in *in vitro* digestibility and available lysine of soy protein isolate after formation of film. *J. Food Eng.* **2004**, *64*, 301−305.

(2) McHugh, T.; Krochta, J. Permeability Properties of Edible Films. In *Edible Coatings and Films to Improve Food Quality*; Krochta, J. M., Baldwin, E. A., Nisperos-Carriedo, M. O, Eds.; Technomic Publishing Co., Inc.: Lancaster, PA, 1994; pp 139−187.

(3) Yang, L.; Paulson, A. T. Effects of lipids on mechanical and moisture barrier properties of edible gellan film. *Food Res. Int.* **2000**, *33*, 571−578.

(4) Liu, X.; Sun, Q.; Wang, H.; Zhang, L. K.; Wang, J. Y. Microspheres of corn protein, zein, for an ivermectin drug delivery system. *Biomaterials* **2005**, *26*, 109−115.

(5) Hurtado-López, P.; Murdan, S. Zein microspheres as drug/antigen carriers: a study of their degradation and erosion, in the presence and absence of enzymes. *J. Microencapsulation* **2006**, *23*, 303−314.

(6) Zhong, Q. X.; Jin, M. F. Nanoscalar structures of spray-dried zein microcapsules and *in vitro* release kinetics of the encapsulated lysozyme as affected by formulations. *J. Agric. Food Chem.* **2009**, *57*, 3886−3894.

(7) Wu, L. Y.; Wen, Q. B.; Yang, X. Q.; Xu, M. S.; Yin, S. W. Wettability, surface microstructure and mechanical properties of films based on phosphorus oxychloride-treated zein. *J. Sci. Food Agric.* **2011**, *91*, 1222−1229.

(8) Fabra, M. J.; Lopez-Rubio, A.; Lagaron, J. M. High barrier polyhydroxyalcanoate food packaging film by means of nanostructured electrospun interlayers of zein. *Food Hydrocolloids* **2013**, *32*, 106−114.

(9) O'Donnell, P. B.; Wu, C. B.; Wang, J. J.; Wang, L.; Oshlack, B.; Chasin, M.; Bodmeier, R.; McGinity, J. W. Aqueous pseudolatex of zein for film coating of solid dosage forms. *Eur. J. Pharm. Biopharm.* **1997**, *43*, 83−89.

(10) Li, K. K.; Yin, S. W.; Yang, X. Q.; Tang, C. H.; Wei, Z. H. Fabrication and characterization of novel antimicrobial films derived from thymol-loaded zein-sodium caseinate (SC) nanoparticles. *J. Agric. Food Chem.* **2012**, *60*, 11592−115600.

(11) Atarés, L.; Bonilla, J.; Chiralt, A. Characterization of sodium caseinate-based edible films incorporated with cinnamon or ginger essential oils. *J. Food Eng.* **2010**, *100*, 678−687.

(12) Fabra, M. J.; Pérez-Masiá, R.; Talens, P.; Chiralt, A. Influence of the homogenization conditions and lipid self-association on properties of sodium caseinate based films containing oleic and stearic acids. *Food Hydrocolloids* **2011**, *25*, 1112−1121.

(13) Pereda, M.; Aranguren, M. I.; Marcovich, N. E. Caseinate films modified with tung oil. *Food Hydrocolloids.* **2010**, *24*, 800−808.

(14) Perez-Gago, M. B.; Krochta, J. M. Lipid particle size effect on water vapour permeability and mechanical properties of whey protein/beeswax emulsion films. *J. Agric. Food. Chem* **2001**, *49*, 996−1002.

(15) Ma, W.; Tang, C. H.; Yin, S. W.; Yang, X. Q.; Qi, J. R.; Xia, N. Effect of homogenization conditions on properties of gelatin−olive oil composite films. *J. Food Eng.* **2012**, *113*, 136−142.

(16) Horn, D.; Rieger, J. Organic nanoparticles in the aqueous phase−theory, experiment, and use. *Angew. Chem., Int. Ed.* **2001**, *40*, 4331−4361.

(17) Chu, B. S.; Ichikawa, S.; Kanafusa, S.; Nakajima, M. Preparation of protein-stabilized beta-carotene nanodispersions by emulsification evaporation method. *J. Am. Oil Chem. Soc.* **2007**, *84*, 1053−1062.

(18) Chu, B. S.; Ichikawa, S.; Kanafusa, S.; Nakajima, M. Preparation and characterization of beta-carotene nanodispersions prepared by solvent displacement technique. *J. Agric. Food. Chem.* **2007**, *55*, 6754−6760.

(19) Tan, C. P.; Nakajima, M. Beta-Carotene nanodispersions: preparation, characterization and stability evaluation. *Food Chem.* **2005**, *92*, 661−671.

(20) Lee, S. J.; McClements, D. J. Fabrication of protein-stabilized nanoemulsions using a combined homogenization and amphiphilic solvent dissolution/evaporation approach. *Food Hydrocolloids* **2010**, *24*, 560−569.

(21) Bouchemal, K.; Briancon, S.; Perrier, E.; Fessi, H. Nano-emulsion formulation using spontaneous emulsification: solvent, oil and surfactant optimization. *Int. J. Pharm.* **2004**, *280*, 241−251.

(22) Dickinson, E. Use of nanoparticles and microparticles in the formation and stabilization of food emulsions. *Trends Food Sci. Technol.* **2012**, *24*, 4−12.

(23) Rockland, L. B. Satured salt solutions for static control of relative humidity between 5 and 40 °C. *Anal. Chem.* **1960**, *32*, 1375−1376.

(24) ASTM. Standard Test Methods for Water Vapor Transmission of Material, Standard Designation: E 96-95. In *Annual Book of ASTM Standards*; American Society for Testing and Materials: Philadelphia, PA, 1995.

(25) McHugh, T. H.; Avena-Bustillos, R.; Krochta, J. M. Hydrophilic edible films: modified procedure for water vapor permeability and explanation of thickness effects. *J. Food Sci.* **1993**, *58*, 899−903.

(26) ASTM. Standard Test Method for Tensile Properties of Thin Plastic Sheeting. Standard Designation: D882. In *Annual Book of ASTM Standards*; American Society for Testing Materials: Philadelphia, PA, 2001.

(27) Ma, W.; Tang, C. H.; Yin, S. W.; Yang, X. Q. Fabrication and characterization of kidney bean (*Phaseolus vulgaris* L.) protein isolate-chitosan composite films at acidic pH. *Food Hydrocolloids* **2013**, *31*, 237−247.

(28) Monedero, F. M.; Fabra, M. J.; Talens, P.; Chiralt, A. Effect of oleic acid beeswax mixtures on mechanical, optical and water barrier properties of soy protein isolate based films. *J. Food Eng.* **2009**, *91*, 509−515.

(29) Morillon, V.; Debeaufort, F.; Blond, G.; Capelle, M.; Voilley, A. Factors affecting the moisture permeability of lipid-based edible films: A review. *Crit. Rev. Food Sci.* **2002**, *42*, 67−89.

(30) Phan The, D.; Debeaufort, F.; Péroval, C.; Despré, D.; Courthaudon, J. L.; Voilley, A. Arabinoxylan-lipids-based edible films and coatings. 3. Influence of drying temperature on film structure and functional properties. *J. Agric. Food. Chem.* **2002**, *50*, 2423−2428.

(31) Vogler, E. A. Structure and reactivity of water at biomaterial surfaces. *Adv. Colloid Interface Sci.* **1998**, *74*, 69−117.

(32) Phan The, D.; Péroval, C.; Debeaufort, F.; Despré, D.; Courthaudon, J. L.; Voilley, A. Arabinoxylan-lipids-based edible films and coatings. 2. Influence of sucroester nature on the emulsion structure and film properties. *J. Agric. Food. Chem.* **2002**, *50*, 266−272.

(33) de Folter, J. W. J.; van Ruijven, M. W. M.; Velikov, K. P. Oil-in-water Pickering emulsions stabilized by colloidal particles from the water-insoluble protein zein. *Soft Matter* **2012**, *8*, 6807−6815.